

RESEARCH

Open Access



Nanomedicine-mediated induction of immunogenic cell death and prevention of PD-L1 overexpression for enhanced hepatocellular carcinoma therapy

Hanzhang Zhu, Weijiang Zhou, Yafeng Wan, Ke Ge, Jun Lu and Changku Jia*

*Correspondence:
jia711222@zju.edu.cn
Department of
Hepatopancreatobiliary
Surgery, Hangzhou
First People's Hospital,
The Affiliated Hospital
of Medical School of
Zhejiang University,
Hangzhou 310006,
Zhejiang, China

Abstract

Background: The present study aims to develop a nanoparticle encapsulating doxorubicin (DOX) and programmed death-ligand 1 (PD-L1) siRNA and evaluate its anti-tumor effects on hepatoma carcinoma (HCC).

Methods: Nanoparticle encapsulating DOX and PD-L1 siRNA (NP_{DOX/siPD-L1}) was characterized by dynamic light scattering and transmission electron microscopy. Flow cytometry was applied to analyze cell populations, NP_{DOX/siPD-L1} internalization, and cell apoptosis. Real-Time (RT)-quantitative reverse transcription (qPCR) and western blotting were used to determine the mRNA and protein levels, respectively. Released ATP was determined using ATP determination kit and cytokines were determined using specific ELISAs. A tumor-bearing animal model was established to evaluate the anti-tumor effects of NP_{DOX/siPD-L1}.

Results: Treatment of NP_{DOX/siPD-L1} induced immunogenic cell death (ICD) and PD-L1 overexpression in HCC. In vivo study demonstrated that intravenously injection of NP_{DOX/siPD-L1} significantly inhibited the tumor volume and PD-L1 expressions of tumor tissue in the H22 tumor-bearing animal model. Besides, the treatment of NP_{DOX/siPD-L1} also regulated the populations of matured dendritic cells and cytotoxic T cells and the productions of cytokines in the tumor tissues.

Conclusion: Taken together, NP_{DOX/siPD-L1} showed significant anti-tumor effects on HCC by the induction of ICD and inhibition of PD-L1 overexpression.

Keywords: Hepatocellular carcinoma, Nanoparticle, Doxorubicin, Immunogenic cell death, PD-L1

Background

Hepatoma, also called hepatocellular carcinoma (HCC), is one of the most frequent malignant cancers worldwide (Bosch et al. 2004). The morbidity and mortality of HCC are globally ranked as third and fifth, respectively. It is known that about 8% of people suffering from hepatitis, who are ease to develop into HCC (Bosch et al. 2004; Sia et al. 2017). Besides, nonalcoholic fatty liver diseases and cirrhosis are also reported to



© The Author(s) 2020. This article is licensed under a Creative Commons Attribution 4.0 International License, which permits use, sharing, adaptation, distribution and reproduction in any medium or format, as long as you give appropriate credit to the original author(s) and the source, provide a link to the Creative Commons licence, and indicate if changes were made. The images or other third party material in this article are included in the article's Creative Commons licence, unless indicated otherwise in a credit line to the material. If material is not included in the article's Creative Commons licence and your intended use is not permitted by statutory regulation or exceeds the permitted use, you will need to obtain permission directly from the copyright holder. To view a copy of this licence, visit <http://creativecommons.org/licenses/by/4.0/>. The Creative Commons Public Domain Dedication waiver (<http://creativecommons.org/publicdomain/zero/1.0/>) applies to the data made available in this article, unless otherwise stated in a credit line to the data.

be associated with the occurrence and development of HCC (Murakami et al. 1998). It is difficult to diagnose HCC at the early stages. There are only 30–40% of patients at HCC early stages who were diagnosed. Once HCC develops into the advanced stages, surgical treatment such as transcatheter arterial chemoembolization becomes less effective, accompanied by poor prognosis and a high recurrence rate (Sia et al. 2017; Bruix et al. 2015). Additionally, surgical treatment is not recommended for patients who had extrahepatic metastases. Thus, chemotherapy is the only option for the treatment of HCC in those patients (Bruix et al. 2015; Li and Wang 2016).

Immunogenic cell death (ICD) is one type of cell death that causes an activation of the immune response (Galluzzi et al. 2017; Garg et al. 2015). When ICD occurs in the tumor microenvironment, calreticulin (CRT) is exposed on the surface of tumor cells, thereby stimulating dendritic cells (DCs) to engulf tumor cells (Galluzzi et al. 2017; Vandenamee et al. 2016; Pitt et al. 2017). In addition, large amounts of adenosine triphosphate (ATP) are released in the tumor tissues, leading to the recruitment of immune cells including monocytes, macrophages, and DCs against tumor-associated antigens (Vandenamee et al. 2016; Showalter et al. 2017). After that, activated cytotoxic T cells mediate the anti-cancer immune responses. Additionally, extracellular High mobility group box 1 protein (HMGB1) has also been implicated to be associated with ICD (Vandenamee et al. 2016; Showalter et al. 2017). HMGB1 is released from the dead cells and is able to bind to toll-like receptor 4, thereby promoting matured DCs to present tumor-associated antigen to the T cells (Vandenamee et al. 2016; Ladoire et al. 2016). These findings encourage us to discover drugs that are able to induce the ICD for cancer therapy.

Many studies have revealed that chemotherapeutic agents including platinum-based drug and doxorubicin (DOX) not only induce cell apoptosis, also trigger ICD (Wong et al. 2015; Fan et al. 2017; Jessup et al. 2019). However, we found that the treatment of DOX enhanced the expressions of programmed death-ligand 1 (PD-L1) in the tumor cells. We inferred that T cell-mediated anti-cancer immune responses were inhibited due to PD-L1 overexpression. To confirm our hypothesis, we evaluated the effects of DOX on the ICD in the PD-L1 knockdown tumor cells. Firstly, we designed a nanoparticle that can encapsulate DOX and PD-L1 siRNA (siPD-L1). Furthermore, to evaluate the anti-tumor effects of the nanoparticle encapsulating DOX and PD-L1 siRNA (NP_{DOX/siPD-L1}) and its underlying mechanisms, we applied HCC cells and tumor-bearing animal models.

Materials and methods

Construction of nanoparticles encapsulating doxorubicin (DOX) and PD-L1 siRNA (NP_{DOX/siPD-L1}) and its characterization

NP_{DOX/siPD-L1} was constructed according to a previously reported method. In brief, block copolymer PEG-PLA (Sigma-Aldrich, St. Louis, MO, USA), cationic lipid DOTAP (Avanti Polar Lipids, Alabaster, AL, USA), and DOX (Sigma-Aldrich) were combined at a ratio of 10:1:1 according to a single emulsion method (Sun et al. 2015). The formed NP_{DOX} was further loaded with PD-L1 siRNA (siPD-L1, Suzhou Ribo Life Science Co., Ltd., Suzhou, China). After that, the gel retardation assay was used to determine the weight ratios of DOTAP to siPD-L1. Dynamic light scattering (DLS, Malvern Zetasizer Nano ZS90) was used to determine particle size and distribution. Transmission electron

microscopy (TEM, JEOL JEM2010 200 kV) was used to observe the size and morphology of NP_{DOX/siPD-L1}.

Cell lines and animals

HCC cell lines including murine H22 and human HepG2 were purchased from the American Type Culture Collection (ATCC, Manassas, VA, USA) and cultured in the complete medium supplied with 10% fetal bovine serum, 100 µg/ml streptomycin, and 100 IU/ml penicillin at 37 °C in the presence of 5% CO₂.

Mouse bone marrow-derived dendritic cells (BMDCs) and human peripheral blood dendritic cells (PBDCs) were isolated and cultured according to previously reported methods (Madaan et al. 2014; Grievink et al. 2016). For BMDCs isolation and culture, bone marrow progenitors were washed out from shin bone and thigh-bone of the mice, then cultured in the medium containing IL-4 (1 ng/ml) and granulocyte-macrophage colony-stimulating factor (10 ng/ml) (PeproTech, Rocky Hill, NJ). After culturing for 48 h, non-adherent cells were gently washed out. The remaining cell clusters were cultured. Medium was changed every other day. On day 7, the cells were collected for further experiments. For PBDCs isolation and culture, PBDCs were purified from non-adherent cells by an iso-osmotic Percoll density gradient, to yield low-density cells. Then, the low-density cells were plated to remove the monocytes. This treatment was repeated. The cells were cultured in the complete culture medium.

In the present study, H22 cells (1×10^6 cells) were co-cultured with BMDCs (1×10^6 cells) at a ratio of 1:1 in the 12-well plates. Similarly, human HepG2 cells (1×10^6 cells) were co-cultured with PBDCs (1×10^6 cells) at a ratio of 1:1 in the 12-well plates. After incubation for 24 h or 48 h, the cells and supernatant were collected for further assays.

H22-OVA cells were constructed by transfecting plasmid encoding OVA (Vector-BUILDER, USA) into H22 cells. OT-1 mice were purchased from the Cyagen Biosciences Inc (Suzhou, China).

Measurement of ATP

After the cells were treated with DOX or nanoparticles for 24 h, the release of ATP was determined using a chemiluminescent ATP determination kit (Life Technologies, Pleasanton, CA, USA), according to the document of the manufacturers.

Flow cytometry

The surface exposure of calreticulin (CRT) was determined using flow cytometry. H22 and HepG2 cells were treated with Doxorubicin (DOX, 0.25 µM) for 24 h and then labeled with anti-CRT-PerCP-Cy5.5 (antibody online. com. Catalog No. ABIN2486728). The percentage of CRT positive cells was quantified based on Propidium iodide (PI) negative cell populations.

To analyze cellular uptake of DOX and PD-L1 siRNA, H22 cells were incubated with indicated antibodies that were labeled with fluorescence Dye. siRNA was labeled with FITC. FITC signal and DOX signal were detected for determining cellular uptake of PD-L1 siRNA and DOX, respectively.

The populations of matured dendritic cells (DCs) and cytotoxic T cells in the tumor tissues were also detected using flow cytometry (BD FACSCalibur, San Jose, CA, USA)

according to a previously reported method (Shang et al. 2018). APC-labeled CD80 (Clone: 16-10A1, BioLegend) and PE-labeled CD86 antibodies were applied to determine the population of DCs. APC-labeled CD4 (Clone: GK1.5, BioLegend) and FITC-labeled CD8 (Clone:53-6.7, BioLegend) were applied to determine the population of cytotoxic T cells. The results were analyzed using software FlowJo (LLC, Ashland, Oregon, USA).

Detection of cell apoptosis

In the present study, cell apoptosis was determined using flow cytometry. Annexin V/PI double staining was applied. H22-OVA cells were treated with nanoparticles for 24 h. Next, the treated H22-OVA cells were co-cultured with CD8+ T cells that were isolated from OT-1 mice in 9 mm petri-dish. Cells were then harvested and suspended in the binding buffer containing FITC-labeled Annexin-V and PI followed by incubation in the dark for 15 min. Then the population of apoptotic cells (Annexin-V⁺PI⁺) was measured by flow cytometry and data were analyzed using software FlowJo.

Quantitative Real-Time reverse transcription(qRT)-PCR

RNA extraction kit was used to isolate RNA from the cells, according to the manufacturer's document. Reverse transcriptase was used in the RT reaction. The Melt curves were used to analyze the accuracy. The expressions of each gene were calculated using $2^{-\Delta\Delta C_t}$ values. The mRNA expression values of PD-L1 were normalized to that of GAPDH.

ELISAs

The supernatant was collected from different treatment groups. The productions of the cytokines including high mobility group box 1 protein (HMGB1), transforming growth factor (TGF)- β , IL12p70, and interferon (IFN)- γ were determined using specific ELISAs according to the manufacturers' instruction (DAKEWE, Beijing, China).

Western blot

The protein was extracted according to the previous methods (Yang et al. 2017). In brief, a cold RIPA buffer containing protease inhibitor was used to lyse the cells or tumor tissues. After that, the extraction buffer was centrifuged at 13,000 g for 10 min to remove the cell debris and other insoluble materials. The BCA protein assay kits were applied to qualify the concentrations of extracted proteins.

An equal amount of proteins was loaded and separated using the 10% SDS gel. After that, the gel was transfer to a PVDF membrane, which was blocked with 5% non-fat milk at room temperature for 2 h. Next, a primary antibody against S-HMGB1 (ab18256, Abcam) or PD-L1 (ab205921, Abcam) was used to incubate with the membrane at 4 °C overnight. Appropriated secondary antibodies conjugated with HRP were used and the imaging system was applied to qualify the expressions of each target proteins. In the present study, bovine serum albumin (BSA) was used as an internal control for soluble HMGB1(S-HMGB1). β -actin was used as an internal control for PD-L1.

H22 tumor-bearing animal model

Murine H22 cells (1×10^7 cells/per mouse) were subcutaneous injected into the C57BL/6 mice. When tumor volumes reached between 50 and 100 mm³, the mice were intravenously injected (*i.v.*) with PBS, NP_{DOX}, NPsiPD-L1, or NP_{DOX/siPD-L1} at every 3 days. The nanoparticles contained DOX at a dose of 2.5 mg/kg and siPD-L1 at a dose of 2 mg/kg. Tumor volumes were recorded every 3 days. Volumes were calculated using an equation [tumor volume (mm³) = (tumor length) × (tumor width)² × 0.5]. At the end of the experimental period, the mice were sacrificed and tumor tissues were collected. The mRNA and protein levels of PD-L1 were measured using qRT-PCR and western blot, respectively. The experimental protocol was supported by the Ethic Commitment of Hangzhou First People's Hospital.

Histopathological analysis

At the end of the experimental period, the mice were sacrificed and the tumor tissues were collected. After the tumor tissues were fixed in 10% formalin solution, the tissues were embedded in paraffin. Hematoxylin and eosin (H&E) staining was performed and the slides were observed under a microscope.

PCNA immunohistochemistry

To analyze the cell proliferation in the tumor tissues, PCNA immunohistochemistry was applied. Paraffin sections were incubated with mouse primary antibody against PCNA followed by incubation with secondary antibody. Avidin–biotin complex procedure was applied. Five randomly chosen sections PCNA immunostained for each group were viewed at a magnification of × 1000 using an image analyzer system.

Statistical analysis

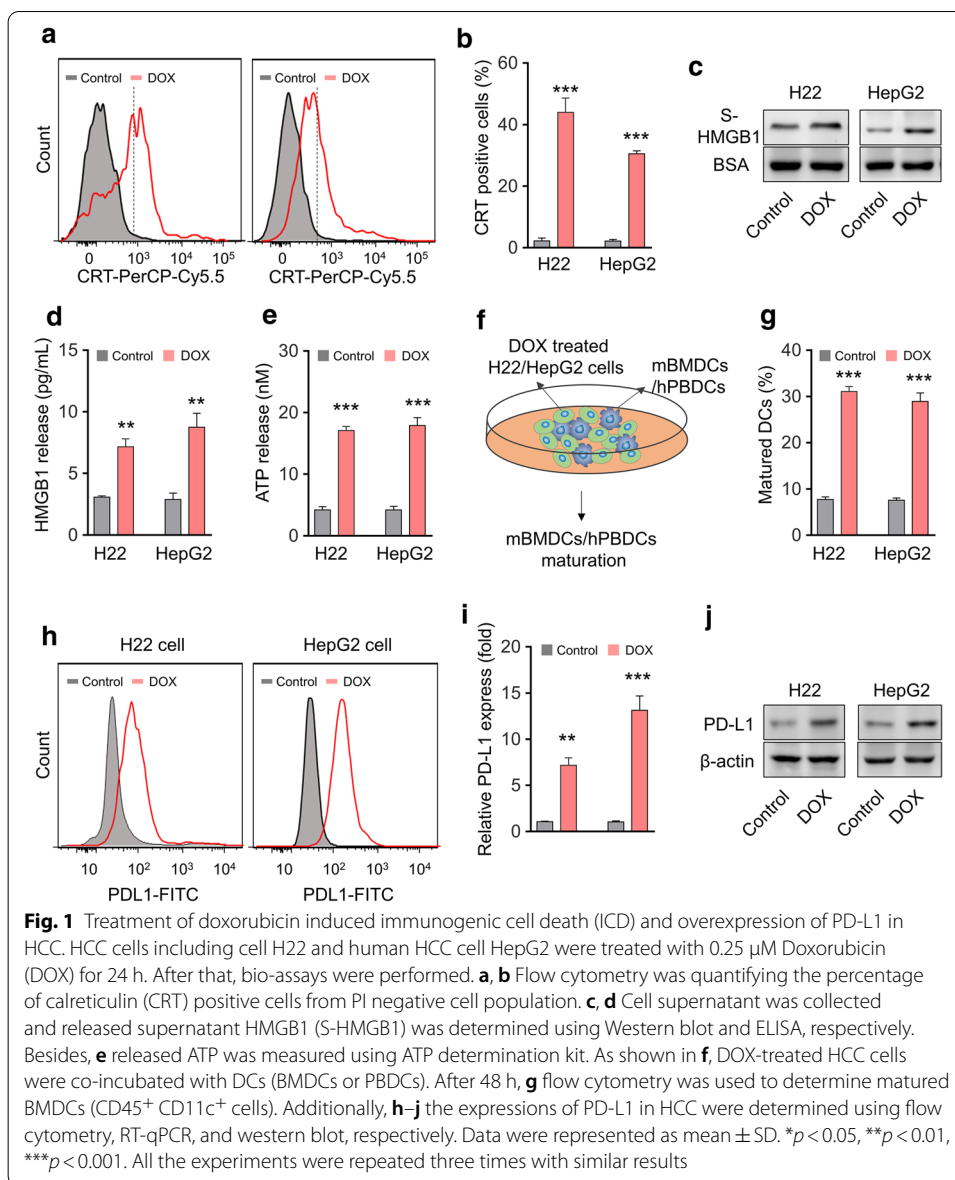
SPSS 13.0 and GraphPad prism were used in this study. Data were shown as mean ± S.D. One- or two-way analysis of variance with multiple comparisons and Student–Newman–Keuls (SNK) test were performed. A *p* value that less than 0.05 was thought as a statistical significance between the two groups.

Results

Treatment of doxorubicin (DOX) induced immunogenic cell death (ICD) and overexpression of PD-L1 in HCC

We explored the effects of DOX on ICD and the expressions of PD-L1 in H22 and HepG2 cells. As shown in Fig. 1a, b, we investigated the effects of DOX on the expressions of CRT, which is responsible for triggering immune cells to kill cancer cells. The results demonstrated that the percentage of CRT positive cells were significantly increased after the cells were treated with DOX. In addition, the results showed that the treatment of DOX significantly increased the release of HMGB1 and ATP when compared with those in the control group (Fig. 1c–e). These results supported that the treatment of DOX induced ICD.

In addition, we co-cultured DOX-treated HCC cells (H22 or HepG2 cells) with DCs (BMDCs or PBDCs). The results showed that the percentage of matured DCs were

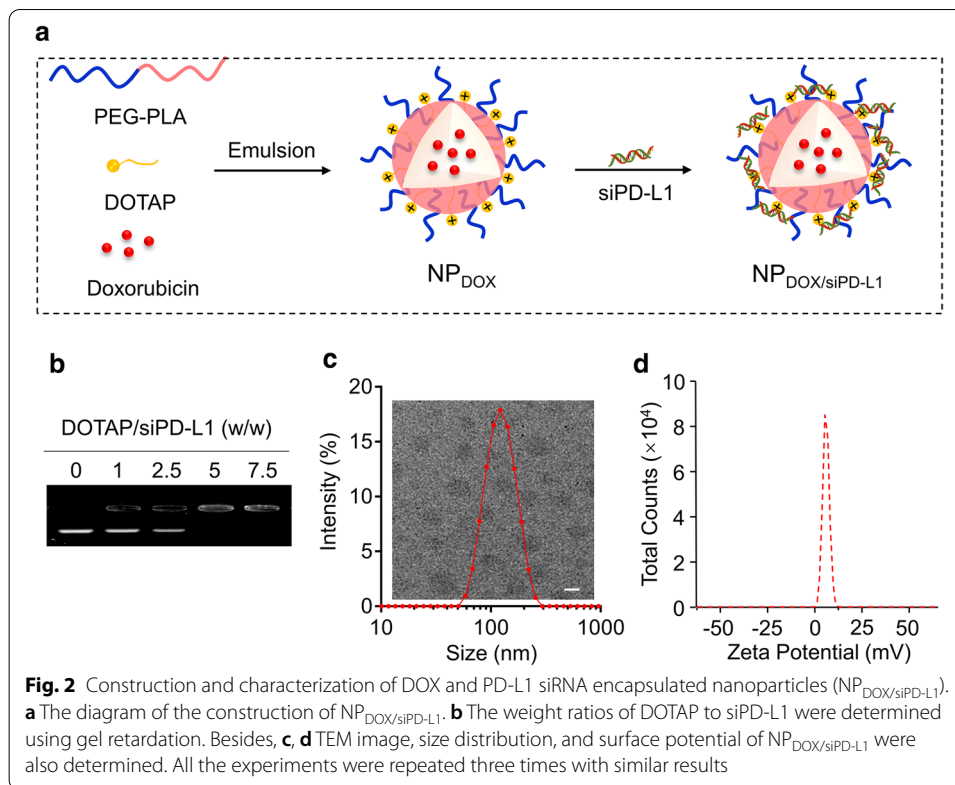


significantly increased when the cells were treated with DOX, indicating the treatment of DOX promoted the mature of DCs (Fig. 1f, g). Furthermore, the frequency of PD-L1 positive cells and the mRNA and protein levels of PD-L1 in HCC cells were significantly increased in the DOX-treated groups (Fig. 1h–j).

Construction and characterization of DOX and PD-L1 siRNA encapsulated nanoparticles

(NP_{DOX/siPD-L1})

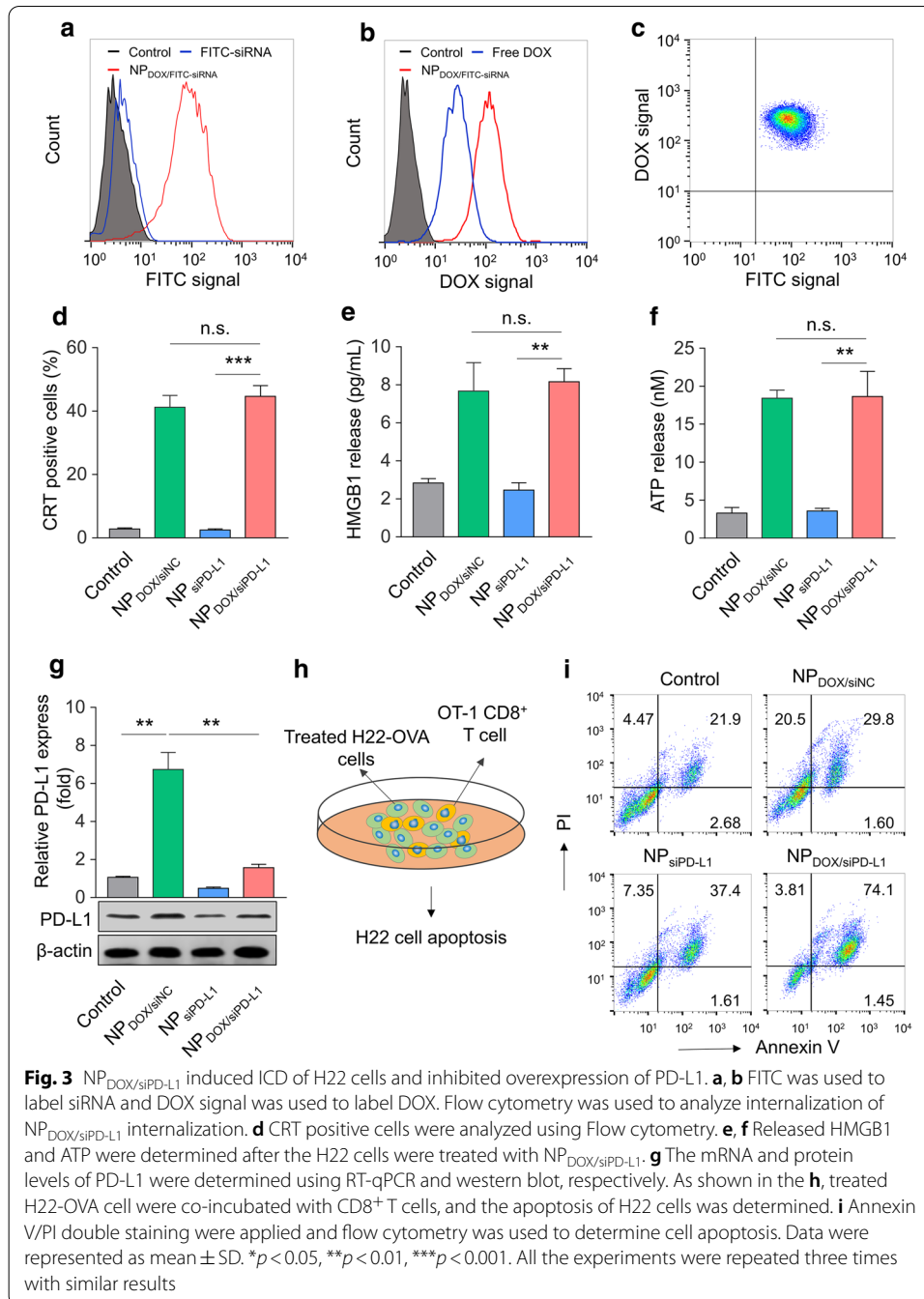
A single emulsion method was used to construct NP_{DOX/siPD-L1}. As shown in Fig. 2a, nanoparticles that were encapsulated with DOX, polyethylene glycol-poly (D,L-lactide) (PEG_{5K}-PLA_{8K}), and cationic lipid DOTAP were mixed at a ratio of 10:1:1 using the emulsion method. Next, the formulated nanoparticles were loaded with PD-L1 siRNA. As shown in Fig. 2b, the gel retardation assay was applied to determine different weight



ratios of DOTAP and siPD-L1. The $NP_{DOX/siPD-L1}$ displayed a uniformed size distribution and a round morphology and its average diameter were equal to 120 nm (Fig. 2c). The zeta potentials of NPDOX and NPDOX/siRNA were about 5.0 and 35.0 mV, respectively (Fig. 2d). The selection of the ratio of PEG-PLA, cationic lipid DOTAP, and DOX was determined according to the encapsulation efficacy of DOX and the surface charge of the obtained nanoparticle. In this ratio, the encapsulation efficacy of DOX could reach 80% and the zeta potential of NPDOX was about 35.0 mV, making it possible to adsorb negative siRNA.

$NP_{DOX/siPD-L1}$ induced ICD of H22 cells and inhibited overexpression of PD-L1

We then determined the effects of $NP_{DOX/siPD-L1}$ on the ICD and the expressions of PD-L1 in the H22 cells. First, we examined the internalization of $NP_{DOX/siPD-L1}$ of the cells. The results demonstrated that both DOX and siPD-L1 were internalized into the cells, indicating the $NP_{DOX/siPD-L1}$ were successfully delivered into the cells (Fig. 3a–c). Next, we determined the effects of $NP_{DOX/siPD-L1}$ on the ICD by evaluation of the frequency of CRT positive cells, and the release of HMGB1 and ATP. The results demonstrated that treatment of $NP_{DOX/siPD-L1}$ significantly increased the frequency of CRT positive cells and the release of HMGB1 and ATP when compared with those in the $NP_{siPD-L1}$ -treated groups (Fig. 3d–f), indicating that the treatment of $NP_{DOX/siPD-L1}$ significantly induced the ICD of H22 cells.



Moreover, to determine the efficiency of PD-L1 siRNA, we measured the mRNA and protein levels of PD-L1 in H22 cells. The results showed that NP_{siPD-L1}- and NP_{DOX/siPD-L1}-treated group significantly decreased the mRNA and protein levels of PD-L1 (Fig. 3g), indicating that PD-L1 siRNA were successfully designed and encapsulated. As shown in Fig. 3h, H22-OVA cells were co-cultured with CD8⁺ T cells that were isolated from OT-1 mice. And then we determined the apoptosis of H22 cells. The results showed that treatment of NP_{DOX/siPD-L1} promoted the apoptotic cell

population when compared with those in the NP_{siPD-L1} or NP_{DOX/siNC}-treated group (Fig. 3i).

NP_{DOX/siPD-L1} existed anti-tumor effects on a H22 tumor-bearing animal model

Before we applied NP_{DOX/siPD-L1} into in vivo study, we firstly determined the stability of NP_{DOX/siPD-L1} in serum. NP_{DOX/siPD-L1} was incubated with fetal bovine serum (10%, v/v)-containing PBS for 72 h and the size of nanoparticles was detected by DLS. As shown in Additional file 1: Fig. S1, a negligible change was observed within 72 h

To confirm the effects of NP_{DOX/siPD-L1} on in vitro study, an H22 tumor-bearing animal model was established to determine the in vivo anti-tumor effects of NP_{DOX/siPD-L1}. Figure 4a displays the experimental schematic H22 tumor-bearing animal model and NP_{DOX/siPD-L1} administration. After subcutaneous injection of H22 cells for 1 week, the nanoparticles were intravenously administrated (*i.v.*) every 3 days. The results showed that tumor volumes in NP_{DOX/siPD-L1} treated groups were significant decreased when compared with those in the NP_{siPD-L1} or NP_{DOX/siNC}-treated groups (Fig. 4b). Next, we determined the mRNA and protein levels of PD-L1 in tumor tissues. The results showed that the mRNA and protein levels of PD-L1 were significantly decreased in the NP_{siPD-L1} or NP_{DOX/siPD-L1} treated group (Fig. 4c, d). Furthermore, histology examination and PCNA were performed. The results showed that the treatment of NP_{DOX/siPD-L1} inhibited cell proliferation in the tumor tissues (Fig. 4e).

Moreover, the present study also investigated the in vivo distribution of NP_{DOX/siPD-L1}. H22 tumor-bearing mice were intravenously administrated with NP_{DOX/siPD-L1} (the

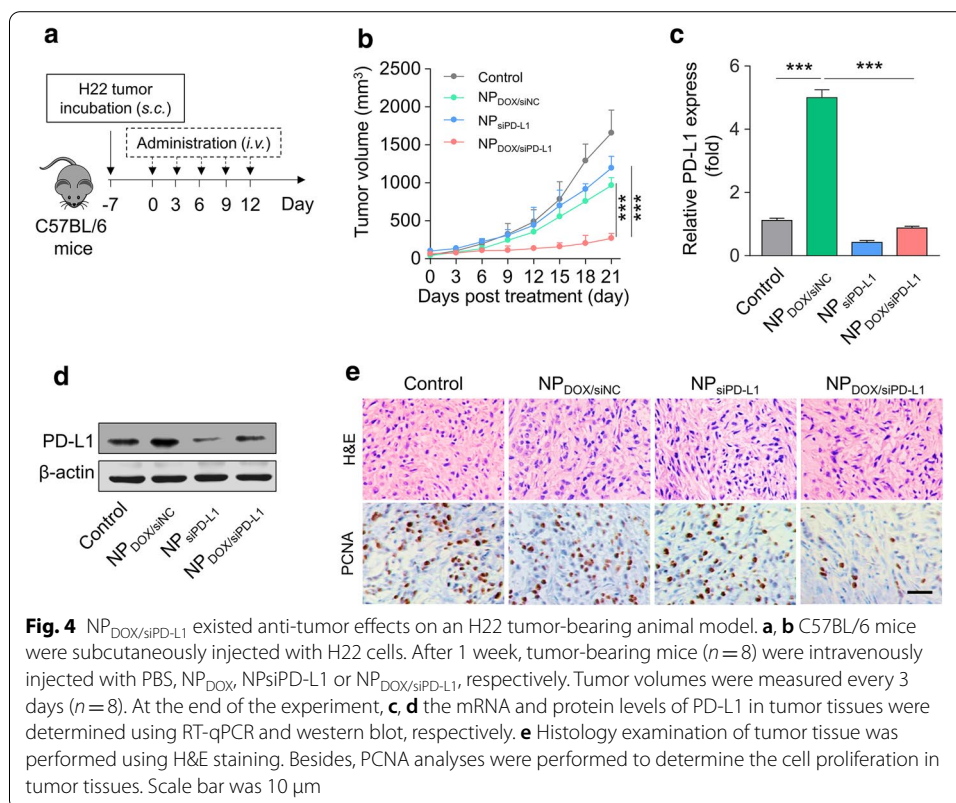
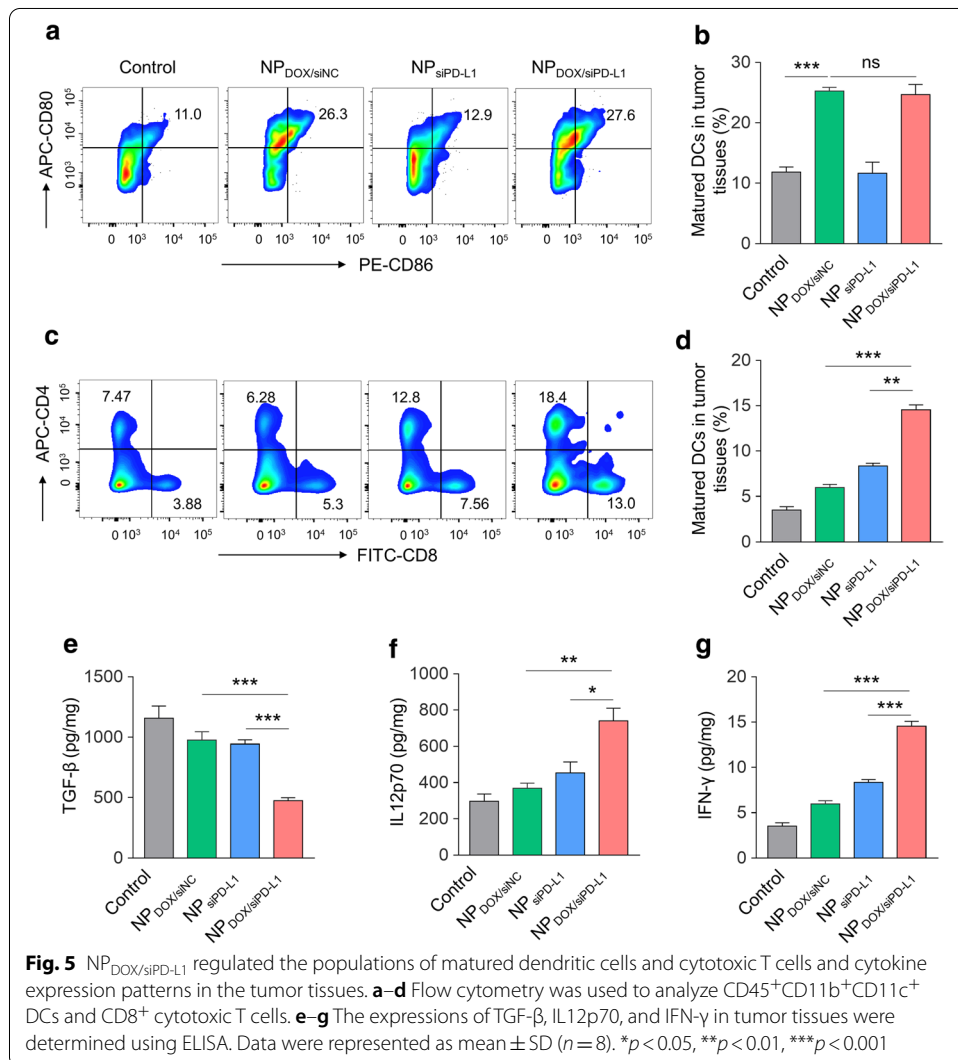


Fig. 4 NP_{DOX/siPD-L1} existed anti-tumor effects on an H22 tumor-bearing animal model. **a, b** C57BL/6 mice were subcutaneously injected with H22 cells. After 1 week, tumor-bearing mice ($n = 8$) were intravenously injected with PBS, NP_{DOX}, NP_{siPD-L1} or NP_{DOX/siPD-L1}, respectively. Tumor volumes were measured every 3 days ($n = 8$). At the end of the experiment, **c, d** the mRNA and protein levels of PD-L1 in tumor tissues were determined using RT-qPCR and western blot, respectively. **e** Histology examination of tumor tissue was performed using H&E staining. Besides, PCNA analyses were performed to determine the cell proliferation in tumor tissues. Scale bar was 10 μ m

injection dose of 2.5 mg/kg), mice were sacrificed 24 h later, main organs and tumor tissues were collected and examined using fluorescence in vivo imaging system (IVIS). We found that NP_{DOX/siPD-L1} efficiently accumulated in tumor tissues, and unavoidably, nanoparticles were also enriched in the spleen, liver, and kidney (Additional file 1: Fig. S2A, B).

NP_{DOX/siPD-L1} regulated the populations of matured dendritic cells and cytotoxic T cells and cytokine expression patterns in the tumor tissues

Finally, we investigated the underlying mechanisms of NP_{DOX/siPD-L1} on its anti-tumor effects. First, we analyzed the percentage of matured dendritic cells and cytotoxic T cells in tumor tissues. The results showed that treatment of NP_{DOX/siNC} or NP_{DOX/siPD-L1} significantly increased the percentage of matured dendritic cells in tumor tissues. However, the treatment of NP_{siPD-L1} did not significantly affect the percentage of matured dendritic cells (Fig. 5a, b). Additionally, NP_{siPD-L1}-treated groups demonstrated a significant increase of the percentage of cytotoxic T cells, and NP_{DOX/siPD-L1}-treated groups



displayed an even higher percentage of cytotoxic T cells in tumor tissues as compared to the NP_{DOX/siPD-L1}-treated groups (Fig. 5c, d).

Moreover, we determined the productions of cytokines including TGF- β , IL12p70, and IFN- γ . The results demonstrated that the productions of TGF- β were significantly decreased in the NP_{DOX/siNC}, NP_{siPD-L1}, or NP_{DOX/siPD-L1}-treated groups in comparison to the control group (Fig. 5e). The NP_{DOX/siPD-L1}-treated groups displayed strong inhibitory effects on the productions of TGF- β . Additionally, the treatment of NP_{DOX/siPD-L1} also showed significant promotion effects on the productions of IL12p70, and IFN- γ (Fig. 5f, g). Taken together, these results supported that the treatment of NP_{DOX/siPD-L1} regulated the populations of matured dendritic cells and cytotoxic T cells and the expressions of cytokines including TGF- β , IL12p70, and IFN- γ in the tumor tissues.

Discussion

In this study, we found that DOX induced ICD in the HCC cells including H22 and HepG2. ICD is characterized by the surface expose of CRT, the release of extracellular HMGB1 and ATP (Garg et al. 2015). Our results demonstrated that the treatment of DOX significantly increased the percentage of CRT positive cells, and the release of extracellular HMGB1 and ATP. Additionally, the release of HMGB1 is a late event of ICD, leading to matured DCs to present tumor-associated antigen to the T cells (Liu et al. 2018; Zhang et al. 2019). We then co-cultured DOX-treated HCC cells with DCs, and the results demonstrated that higher amount of matured DCs in the DOX-treated treated group as compared with those in the control group. These results supported that the treatment of DOX induced ICD in the HCC, which are consistent with a previous finding, in which DOX not only induces cell apoptosis, also triggers ICD (Kawano et al. 2016). However, the treatment of DOX enhanced the expressions of PD-L1 in the tumor cells. It is known that PD-L1 binds to programmed cell death protein 1 (PD-1), a co-inhibitor expressed on T cell surface that regulates T cell-mediated immune response (Zou et al. 2016; Roemer et al. 2016). Overexpression of PD-L1 is an obstacle for the treatment of DOX. Therefore, the present study aims to explore the effects of DOX on the ICD when it comes to that PD-L1 was inhibited.

Pegylated liposomal doxorubicin has been approved by the Food and Drug Administration (FDA) in 1995 (Hadjidemetriou et al. 2016). Since then, nanoparticle-based delivery systems for the DOX have drawn much attention in recent years (Jain et al. 2015; Malinovskaya et al. 2017). In the present study, we developed NP_{DOX/siPD-L1} in two steps. First, we mixed nanoparticles that were encapsulated with DOX, polyethylene glycol-poly (D,L-lactide) (PEG_{5K}-PLA_{8K}), and cationic lipid DOTAP at a ratio of 10: 1: 1 using the emulsion method. Second, we loaded siPD-L1 into the formulated nanoparticles. Our results demonstrated that the NP_{DOX/siPD-L1} displayed a uniformed size distribution and a round morphology. Additionally, both DOX and siPD-L1 were internalized into the cells, indicating NP_{DOX/siPD-L1} successfully being delivered the cells.

Overexpression of PD-L1 on the cancer cells promote cancer cell escape from T cell-mediated immune response (Tang et al. 2018). The previous study has demonstrated that the blockage of PD-L1 is an effectively adjunctive strategy to boost ICD (Tang et al. 2018). In this study, we observed that the knockdown of PD-L1 did not impact the ICD events including the expressions of CRT, the release of extracellular HMGB1 and ATP.

Interestingly, when we combined DOX and siPD-L1, the results showed that treatment of NP_{DOX/siPD-L1} significantly increased the frequency of CRT positive cells and the release of HMGB1 and ATP when compared with those in the NP_{siPD-L1}-treated groups. These results supported the adjunctive role of blocking PD-L1 in the augment of ICD. Furthermore, we co-cultured treated H22-OVA cells with CD8⁺ T cells and evaluated the effects of NP_{siPD-L1} and NP_{DOX/siPD-L1} on the cell apoptosis. CD8⁺ T cells are also known as cytotoxic T cells, which have been indicated to play a crucial role in cancer cell surveillance. In the present study, we found that the treatment of NP_{siPD-L1} or NP_{DOX/siPD-L1} promoted HCC cell apoptosis.

To confirm the anti-tumor effects of NP_{DOX/siPD-L1} in vitro, an H22 tumor-bearing animal model was established. First, the results showed that the expressions of PD-L1 were significantly decreased in the NP_{siPD-L1} or NP_{DOX/siPD-L1} treated group, indicating that the DOX and siPD-L1 were successfully delivered by nanoparticles. Surprisingly, the results showed a significant decrease in tumor volume in NP_{DOX/siPD-L1} treated groups. These results are consistent with PCNA analysis, in which showed that cell proliferation in tumor tissues was inhibited in the NP_{DOX/siPD-L1} treated group. We then explored whether the anti-tumor effects of NP_{DOX/siPD-L1} were associated with the regulation of the population of immune cells. Two types of cells including matured DCs and CD8⁺ T cells were analyzed in the tumor tissues. Matured DCs are known to present antigen to the T cells, whilst CD8⁺ T cells are known to kill cancer cells (Gardner and Ruffell 2016; Wang et al. 2019). Our results showed that NP_{DOX/siPD-L1} significantly increased the percentage of matured dendritic cells and CD8⁺ T cells in tumor tissues, indicating NP_{DOX/siPD-L1} regulated the populations of matured DCs and CD8⁺ T cells. Additionally, we also evaluated the productions of classic cytokines including TGF- β , IL12p70, and IFN- γ . It is known that CD8⁺ T cells secrete cytokines including IFN- γ which have anti-tumor functions (Wang et al. 2019; Gao et al. 2017). IL12p70, a cytokine produced by DCs, has been reported to trigger the activation of CD8⁺ T cells by the production of chemokines. (Lu 2017) It has been reported that TGF- β regulates T cell differentiation (Colak and Ten Dijke 2017). The results demonstrated that NP_{DOX/siPD-L1}-treated groups inhibited the productions of TGF- β and promoted the productions of IL12p70 and IFN- γ . In summary, these results supported that the treatment of NP_{DOX/siPD-L1} existed anti-tumor effects by the regulation of the populations of matured DCs and CD8⁺ T cells and the expressions of cytokines including TGF- β , IL12p70, and IFN- γ .

Conclusion

In the present study, for the first time, we successfully developed a NP_{DOX/siPD-L1} that is able to simultaneously deliver DOX and PD-L1 siRNA into HCC cells and tumor tissues. Our results demonstrated that the treatment of NP_{DOX/siPD-L1} significantly induced ICD in the HCC cells. Additionally, in vivo study supported that treatment of NP_{DOX/siPD-L1} significantly inhibited tumor growth in part by the regulation the populations of matured DCs and cytotoxic T cells and the expressions of cytokines including TGF- β , IL12p70, and IFN- γ .

Supplementary information

Supplementary information accompanies this paper at <https://doi.org/10.1186/s12645-020-00072-6>.

Additional file 1. Figure S1 and S2.

Abbreviations

DOX: Doxorubicin; HCC: Hepatoma carcinoma; ICD: Immunogenic cell death; CRT: Calreticulin; DCs: Dendritic cells; PD-L1: Programmed death-ligand 1; ATP: Adenosine triphosphate; HMGB1: High mobility group box 1 protein; S-HMGB1: Soluble HMGB1; siPD-L1: PD-L1 siRNA; NP_{DOX/siPD-L1}: Nanoparticles encapsulating DOX and PD-L1 siRNA; FDA: Food and Drug Administration; TGF: Transforming growth factor; IFN: Interferon; BMDCs: Mouse bone marrow-derived dendritic cells; PBDCs: Human peripheral blood dendritic cells; H&E: Hematoxylin and eosin; PI: Propidium iodide.

Acknowledgements

None.

Authors' contributions

Conception/design: HZ, WZ, YW, KG, JL and CJ. Collection and/or assembly of data: WZ, YW, KG and JL. Manuscript writing: HZ and CJ. Final approval of manuscript: HZ, WZ, YW, KG, JL and CJ. All authors read and approved the final manuscript.

Funding

This work was supported by grants from Medicine and Health Science and Technology Plan Projects of Zhejiang Province (grant No. 2021KY231) and Zhejiang Provincial Natural Science Foundation of China (grant No. LY21H160016).

Availability of data and materials

The datasets used and/or analyzed during the current study are available from the corresponding author on reasonable request.

Ethics approval and consent to participate

The experimental protocol was supported by the Ethic Commitment of Hangzhou First People's Hospital.

Consent for publication

Current study is available from the corresponding author on reasonable request.

Competing interests

All of the authors declare that they have no competing interests.

Received: 14 August 2020 Accepted: 1 December 2020

Published online: 14 December 2020

References

- Bosch FX, Ribes J, Diaz M, Cleries R. Primary liver cancer: worldwide incidence and trends. *Gastroenterology*. 2004;127:S5–16. <https://doi.org/10.1053/j.gastro.2004.09.011>.
- Bruix J, Han KH, Gores G, Llovet JM, Mazzaferro V. Liver cancer: approaching a personalized care. *J Hepatol*. 2015;62:S144–56. <https://doi.org/10.1016/j.jhep.2015.02.007>.
- Colak S, Ten Dijke P. Targeting TGF-beta signaling in cancer. *Trends Cancer*. 2017;3:56–71. <https://doi.org/10.1016/j.trecan.2016.11.008>.
- Fan Y, Kuai R, Xu Y, Ochyl LJ, Irvine DJ, Moon JJ. Immunogenic cell death amplified by co-localized adjuvant delivery for cancer immunotherapy. *Nano Lett*. 2017;17:7387–93. <https://doi.org/10.1021/acs.nanolett.7b03218>.
- Galluzzi L, Buque A, Kepp O, Zitvogel L, Kroemer G. Immunogenic cell death in cancer and infectious disease. *Nat Rev Immunol*. 2017;17:97–111. <https://doi.org/10.1038/nri.2016.107>.
- Gao Z, Li Y, Wang F, Huang T, Fan K, Zhang Y, Zhong J, Cao Q, Chao T, Jia J, Yang S, Zhang L, Xiao Y, Zhou JY, Feng XH, Jin J. Mitochondrial dynamics controls anti-tumour innate immunity by regulating CHIP-IRF1 axis stability. *Nat Commun*. 2017;8:1805. <https://doi.org/10.1038/s41467-017-01919-0>.
- Gardner A, Ruffell B. Dendritic cells and cancer immunity. *Trends Immunol*. 2016;37:855–65. <https://doi.org/10.1016/j.it.2016.09.006>.
- Garg AD, Dudek-Peric AM, Romano E, Agostinis P. Immunogenic cell death. *Int J Dev Biol*. 2015;59:131–40. <https://doi.org/10.1387/ijdb.150061pa>.
- Grievink HW, Luisman T, Klufft C, Moerland M, Malone KE. Comparison of Three Isolation Techniques for Human Peripheral Blood Mononuclear Cells: cell Recovery and Viability, Population Composition, and Cell Functionality. *Biopreserv Biobank*. 2016;14:410–5. <https://doi.org/10.1089/bio.2015.0104>.
- Hadjidemetriou M, Al-Ahmady Z, Kostarelos K. Time-evolution of in vivo protein corona onto blood-circulating PEGylated liposomal doxorubicin (DOXIL) nanoparticles. *Nanoscale*. 2016;8:6948–57. <https://doi.org/10.1039/c5nr09158f>.
- Jain A, Kesharwani P, Garg NK, Jain A, Jain SA, Jain AK, Nirbhavane P, Ghanghoriya R, Tyagi RK, Katara OP. Galactose engineered solid lipid nanoparticles for targeted delivery of doxorubicin. *Colloids Surf B Biointerfaces*. 2015;134:47–58. <https://doi.org/10.1016/j.colsurfb.2015.06.027>.
- Jessup JM, Kabbout M, Korokhov N, Joun A, Tollefson AE, Wold WSM, Mattoo AR. Adenovirus and Oxaliplatin cooperate as agnostic sensitizers for immunogenic cell death in colorectal carcinoma. *Hum Vaccin Immunother*. 2019. <https://doi.org/10.1080/21645515.2019.1665960>.
- Kawano M, Tanaka K, Itonaga I, Iwasaki T, Miyazaki M, Ikeda S, Tsumura H. Dendritic cells combined with doxorubicin induces immunogenic cell death and exhibits antitumor effects for osteosarcoma. *Oncol Lett*. 2016;11:2169–75. <https://doi.org/10.3892/ol.2016.4175>.

- Ladoire S, Enot D, Andre F, Zitvogel L, Kroemer G. Immunogenic cell death-related biomarkers: impact on the survival of breast cancer patients after adjuvant chemotherapy. *Oncoimmunology*. 2016;5:e1082706. <https://doi.org/10.1080/2162402X.2015.1082706>.
- Li L, Wang H. Heterogeneity of liver cancer and personalized therapy. *Cancer Lett*. 2016;379:191–7. <https://doi.org/10.1016/j.canlet.2015.07.018>.
- Liu P, Zhao L, Loos F, Iribarren K, Kepp O, Kroemer G. Epigenetic anticancer agents cause HMGB1 release in vivo. *Oncoimmunology*. 2018;7:e1431090. <https://doi.org/10.1080/2162402X.2018.1431090>.
- Lu X. Impact of IL-12 in cancer. *Curr Cancer Drug Targets*. 2017;17:682–97. <https://doi.org/10.2174/1568009617666170427102729>.
- Madaan A, Verma R, Singh AT, Jain SK, Jaggi M. A stepwise procedure for isolation of murine bone marrow and generation of dendritic cells. *Journal of Biological Methods*. 2014;1:e1.
- Malinovskaya Y, Melnikov P, Baklaushev V, Gabashvili A, Osipova N, Mantrov S, Ermolenko Y, Maksimenko O, Gorshkova M, Balabanyan V, Kreuter J, Gelperina S. Delivery of doxorubicin-loaded PLGA nanoparticles into U87 human glioblastoma cells. *Int J Pharm*. 2017;524:77–90. <https://doi.org/10.1016/j.ijpharm.2017.03.049>.
- Murakami T, Kim T, Nakamura H. Hepatitis, cirrhosis, and hepatoma. *J Magn Reson Imaging*. 1998;8:346–58. <https://doi.org/10.1002/jmri.1880080214>.
- Pitt JM, Kroemer G, Zitvogel L. Immunogenic and Non-immunogenic Cell Death in the Tumor Microenvironment. *Adv Exp Med Biol*. 2017;1036:65–79. https://doi.org/10.1007/978-3-319-67577-0_5.
- Roemer MG, Advani RH, Ligon AH, Natkunam Y, Redd RA, Homer H, Connelly CF, Sun HH, Daadi SE, Freeman GJ, Armand P, Chapuy B, de Jong D, Hoppe RT, Neuberg DS, Rodig SJ, Shipp MA. PD-L1 and PD-L2 genetic alterations define classical hodgkin lymphoma and predict outcome. *J Clin Oncol*. 2016;34:2690–7. <https://doi.org/10.1200/JCO.2016.66.4482>.
- Shang W, Jiang Y, Boettcher M, Ding K, Mollenauer M, Liu Z, Wen X, Liu C, Hao P, Zhao S. Genome-wide CRISPR screen identifies FAM49B as a key regulator of actin dynamics and T cell activation. *Proc Natl Acad Sci*. 2018;115:E4051–60.
- Showalter A, Limaye A, Oyer JL, Igarashi R, Kittipatarin C, Copik AJ, Khaled AR. Cytokines in immunogenic cell death: applications for cancer immunotherapy. *Cytokine*. 2017;97:123–32. <https://doi.org/10.1016/j.cyto.2017.05.024>.
- Sia D, Villanueva A, Friedman SL, Llovet JM. Liver cancer cell of origin, molecular class, and effects on patient prognosis. *Gastroenterology*. 2017;152:745–61. <https://doi.org/10.1053/j.gastro.2016.11.048>.
- Sun R, Liu Y, Li SY, Shen S, Du XJ, Xu CF, Wang J. Co-delivery of all-trans-retinoic acid and doxorubicin for cancer therapy with synergistic inhibition of cancer stem cells. *J Control Release*. 2015;213:e94. <https://doi.org/10.1016/j.jconrel.2015.05.156>.
- Tang H, Liang Y, Anders RA, Taube JM, Qiu X, Mulgaonkar A, Liu X, Harrington SM, Guo J, Xin Y. PD-L1 on host cells is essential for PD-L1 blockade-mediated tumor regression. *J Clin Invest*. 2018;128:580–8.
- Vandenabeele P, Vandecasteele K, Bachert C, Krysko O, Krysko DV. Immunogenic Apoptotic Cell Death and Anticancer Immunity. *Adv Exp Med Biol*. 2016;930:133–49. https://doi.org/10.1007/978-3-319-39406-0_6.
- Wang W, Green M, Choi JE, Gijon M, Kennedy PD, Johnson JK, Liao P, Lang X, Kryczek I, Sell A, Xia H, Zhou J, Li G, Li J, Li W, Wei S, Vatan L, Zhang H, Szeliga W, Gu W, Liu R, Lawrence TS, Lamb C, Tanno Y, Cieslik M, Stone E, Georgiou G, Chan TA, Chinnaiyan A, Zou W. CD8(+) T cells regulate tumour ferroptosis during cancer immunotherapy. *Nature*. 2019;569:270–4. <https://doi.org/10.1038/s41586-019-1170-y>.
- Wong DY, Ong WW, Ang WH. Induction of immunogenic cell death by chemotherapeutic platinum complexes. *Angew Chem Int Ed Engl*. 2015;54:6483–7. <https://doi.org/10.1002/anie.201500934>.
- Yang H, Wang J, Fan JH, Zhang YQ, Zhao JX, Dai XJ, Liu Q, Shen YJ, Liu C, Sun WD, Sun Y. Ilexgenin A exerts anti-inflammation and anti-angiogenesis effects through inhibition of STAT3 and PI3K pathways and exhibits synergistic effects with Sorafenib on hepatoma growth. *Toxicol Appl Pharmacol*. 2017;315:90–101. <https://doi.org/10.1016/j.taap.2016.12.008>.
- Zhang Y, Liu RB, Cao Q, Fan KQ, Huang LJ, Yu JS, Gao ZJ, Huang T, Zhong JY, Mao XT, Wang F, Xiao P, Zhao Y, Feng XH, Li YY, Jin J. USP16-mediated deubiquitination of calcineurin A controls peripheral T cell maintenance. *J Clin Invest*. 2019;129:2856–71. <https://doi.org/10.1172/JCI123801>.
- Zou W, Wolchok JD, Chen L. PD-L1 (B7-H1) and PD-1 pathway blockade for cancer therapy: mechanisms, response biomarkers, and combinations. *Sci Transl Med*. 2016;8:328rv324. <https://doi.org/10.1126/scitranslmed.aad7118>.

Publisher's Note

Springer Nature remains neutral with regard to jurisdictional claims in published maps and institutional affiliations.

Ready to submit your research? Choose BMC and benefit from:

- fast, convenient online submission
- thorough peer review by experienced researchers in your field
- rapid publication on acceptance
- support for research data, including large and complex data types
- gold Open Access which fosters wider collaboration and increased citations
- maximum visibility for your research: over 100M website views per year

At BMC, research is always in progress.

Learn more biomedcentral.com/submissions

